

Uniform magnetization rotation in single ferromagnetic nanowires

Y. Jaccard,* Ph. Guittienne, D. Kelly, J.-E. Wegrowe, and J.-Ph. Ansermet
*Ecole Polytechnique Fédérale de Lausanne (EPFL), Institut de Physique Expérimentale (IPE), PhB-Ecublens,
 1015 Lausanne, Switzerland*

(Received 22 September 1999; revised manuscript received 25 February 2000)

Using electrochemical deposition, 6 μm long Ni nanowires, with typical diameters of the order of 80 nm, are grown in ion-track etched membranes. Electrical contacts are established during the growth, allowing measurements of single wires. The full magnetoresistive hysteresis loop is studied as a function of the angle between the applied field and the wire direction. For each field sweep, a discontinuity is observed. It corresponds to the irreversible switching of the magnetization. A model of uniform reversal of the magnetization accounts for the reversible part of these magnetoresistive loops using the conventional $\cos^2\omega$ dependence of the resistance with the angle ω defined between magnetization and electric current. The angular dependence of the switching field is discussed.

I. INTRODUCTION

The recent development of techniques allowing the fabrication and the measurement of submicrometric structures has given renewed interest in studying their magnetic properties especially when the dimensions become comparable to a characteristic length scale of the material, such as the domain-wall width. Thus the magnetic order and the magnetization reversal process of such structures are expected to show interesting behavior which could be explained with micromagnetic models. From the applied physics point of view, the continuous increase in the density of magnetic recording media implies a good knowledge of the behavior of these submicrometric ferromagnetic structures.

Compared to e-beam lithography,¹⁻³ electrodeposition in nanoporous membranes is a relatively simple and inexpensive way of producing magnetic systems of submicrometric structures. This technique is particularly suitable for the production of long cylinders with diameter less than 100 nm.⁴⁻⁶

Previous studies on isolated, long ferromagnetic cylinders^{4,7} focused on the irreversible part of the magnetization reversal, the so-called switching field, because of the experimental difficulties of measuring very small changes of magnetization (less than 10^{-14} A m²). In contrast, the magnetoresistive measurement has been shown to be a good alternative way to get information on the whole reversal process of the magnetization of mesoscopic structures.⁸ Recently, it became possible to detect the full magnetization curve of such cylinder using either micro-SQUID's (Ref. 9) or resistive measurements.¹⁰⁻¹²

In this paper, we present a detailed study of the angular dependence of the magnetoresistance of single nickel nanowires. About 20 single wires have been systematically studied. The data shown in this paper were taken with two of them and referred to as sample A and B. Such wires have a predominant shape anisotropy. The observed anisotropic magnetoresistance (AMR) is of the order of magnitude of that of bulk Ni. This shows that the contact resistance is low. The diameter of the wires, of the order of 80 nm, is comparable to the domain wall thickness of Ni. The magnetoresistance of such wires looks qualitatively different in comparison with

the magnetoresistance of wires with larger diameters in which the presence of magnetic domains can be expected, as observed by Jia *et al.*¹⁰ Therefore we could hope to get single domain behavior in these wires of the order of 80 nm in diameter. Indeed we found, as will be shown, that a model of uniform magnetization reversal accounts for the reversible part of the magnetoresistive loops considering a large anisotropy in the wire direction, as previously inferred from other measurements.¹²⁻¹⁴ On the contrary, considering the obtained results in this reversible regime, the angular dependence of the switching field (related to the magnetization reversal in the irreversible regime) may not be described by the micromagnetic models of Stoner-Wohlfarth or Curling. However, the angular dependence of this irreversible reversal may be defined as a Curling reversal by taking into account a smaller volume than the one, which rotates uniformly. Possible explanations are discussed.

II. SAMPLE PREPARATION AND MEASUREMENT

Ferromagnetic polycrystalline nanowires of Ni were produced by electrodeposition in commercial nanoporous membranes¹⁵ of 6 μm in thickness. The pores are not perfectly aligned perpendicular to the membrane. The distribution of the angle between the pore axis and the normal to the plane of the membrane ranges over 17° as specified by the membrane manufacturer.¹⁵ The pore density of 6×10^8 cm⁻² is low enough that the wires are magnetically decoupled.¹³ The wire diameters are distributed around an average of 80 ± 20 nm, as measured by transmission electron microscopy.¹⁶ Individual nanowires were electrically contacted with a newly developed technique,¹⁷ thus making possible the study of magnetization reversal in single nanowires. To obtain single contacts on such a density of pores with a good reliability, the technique was improved by depositing on each face of the membrane well-defined gold thicknesses in order to select a smaller range of diameters. For that, the gold electrode (bottom layer) was covered with silver paint. Due to the grain size of silver paint, only the solvent penetrates and closes by drying the pores not fully covered by the gold layer (Fig. 1). As a consequence, the effective pore

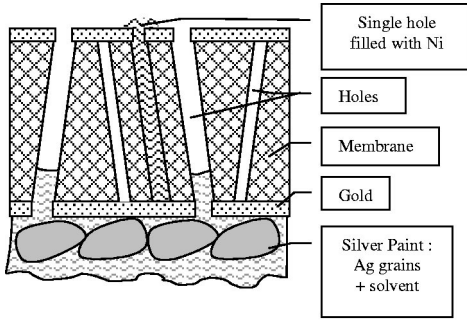


FIG. 1. Schematics of the improved technique in order to get a single contact.

density was reduced and the probability of establishing a single contact increased.

Resistive measurements as a function of temperature were done to characterize the Ni wires resistance. Following the Mathiessen law, the resistivity may be deduced from the variation of resistance with temperature and from comparison with tabulated values.¹⁸ Typical resistance values, at room temperature and zero applied field, for Ni single wires, were measured in the range $R_0 = 100\text{--}200\ \Omega$. A lower limit for their resistivity of $\rho = 13\ \mu\Omega\ \text{cm}$ was thus obtained. Moreover, magnetoresistive measurements gave a typical AMR ratio of the order of $\Delta R/R_0 = (R_0 - R_{\text{sat}})/R_0 = 1.5\%$ where R_{sat} is the resistance at the field corresponding to a saturated magnetization perpendicular to the wire. These two values are close to what has been obtained for polycrystalline films¹⁹ and hints to the quality of the improved single contacts.¹²

Using an ac technique, magnetotransport measurements were performed with low excitation currents ($j \approx 2 \times 10^4\ \text{A cm}^{-2}$) at room temperature on a manually rotating sample holder (precision of 2°). Typical voltage noise on measurements is around 40 nV. The electromagnet in a Helmholtz coil configuration could reach a maximum applied field of $\mu_0 H = 0.7\ \text{T}$ with a minimum field step of 0.2 mT. The field was measured using a transverse Hall probe.

III. MAGNETIZATION REVERSAL IN INDIVIDUAL NANO-SIZED FERROMAGNETIC WIRES

The anisotropic magnetoresistance (AMR), being an effect due to the anisotropy of spin-orbit scattering, depends on the angle between the current and the magnetization. For a long single domain wire, the AMR can be expressed as being proportional to $\cos^2 \omega$ ^{19,20} where ω is defined as the angle between the magnetization and the wire axis because ω is the same as the angle between magnetization and current in this case. This gives the following expression for the AMR:

$$R(\mu_0 H, \Omega) = R_{\perp} + \Delta R \cos^2 \omega, \quad (1)$$

where Ω is the angle between the applied field $\mu_0 H$ and the wire axis, R_{\perp} is the resistance when the saturated magnetization is perpendicular to the current and $\Delta R = R_{//} - R_{\perp}$ with $R_{//}$, the resistance when the saturated magnetization is parallel to the current. In our case, we get $R_{//} = R(\mu_0 H_{\text{sat}}, \Omega = 0^\circ)$ and $R_{\perp} = R(\mu_0 H_{\text{sat}}, \Omega = 90^\circ)$ with $\mu_0 H_{\text{sat}}$, the applied field necessary to saturate the magnetization in any direction.

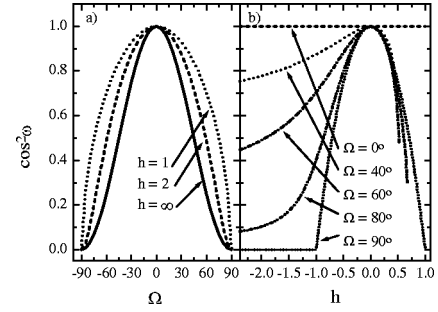


FIG. 2. Considering Eq. (2) for explaining the AMR, representation of $\cos^2 \omega$ versus (a) Ω for different values of h and (b) h for different values of Ω .

The data were analyzed with the simple model of Stoner-Wohlfarth²¹ of uniform rotation. For the sake of clarity, the main formula of this well-known model, used in the paper, are summarized in the Appendix.

In order to get a relation between $\cos^2 \omega$, the normalized field $h = \mu_0 H / \mu_0 H_a$ and the angle Ω , the following equation has to be solved [see Eq. (A1) with the definitions below]:

$$(\cos^2 \omega - 1)(\cos \omega + h \cos \Omega)^2 + (h \sin \Omega)^2 \cos^2 \omega = 0. \quad (2)$$

The dependencies of $\cos^2 \omega$ on Ω for different fixed h and on h for different fixed Ω are shown in Figs. 2(a) and 2(b), respectively.

The distribution in the orientation of the pores forces to use two angles to define the orientation of the wire with respect to the plane of the applied field rotation (Fig. 3). We use ϵ , the complement to the polar angle and α , the azimuthal angle. The real angle Ω between the applied field and the wire direction is then given by

$$\cos \Omega = \cos \epsilon \cos \alpha. \quad (3)$$

The angular dependence of single wires resistance was first measured at the maximum field of the magnet ($\mu_0 H = 0.7\ \text{T}$) in order to determine the azimuthal angle value α [Fig. 4(a)]. Then magnetoresistive curves were measured for different values of this angle α [Fig. 4(b)]. Because of the symmetry of the curves (no measurable hysteresis loops) and of the identical resistance at zero field for the longitudinal and transverse direction, the nonzero magnetoresistance

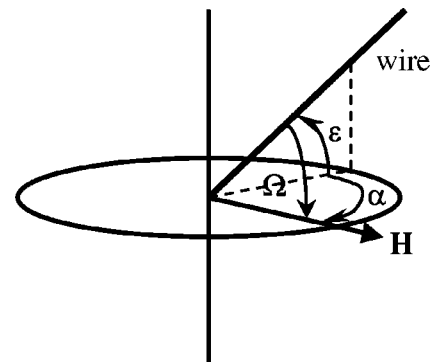


FIG. 3. Angles necessary to give the orientation of the measured wire with respect to the plane defined by the rotation of the applied field $\mu_0 H$.

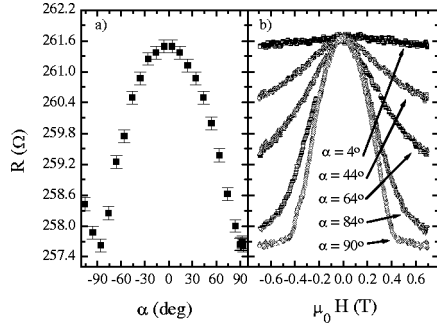


FIG. 4. (a) Angular dependence α of a single Ni wire's resistance (sample A) at the maximum field of the magnet, i.e., $\mu_0 H_{\max} = 0.7$ T. The angle α is defined as the azimuthal angle between the plane of applied field rotation and the wire axis (see Fig. 3). (b) Magneto-resistance of this wire for different angles α .

change at $\alpha = 0^\circ$ is related to the experimental difficulty to align the wires axis with the field. Among the twenty measured samples, none have shown such a zero magneto-resistance change. One of the possible reasons is the improvement of the fabrication process. Indeed, the gold layer is not thick enough to close the pores perfectly perpendicular to the membrane surface. Only the off-axis ones are closed.

In the following, we present a reliable procedure which demonstrates the excellent match of the predictions of the model (Fig. 2) to our experimental data (Fig. 4) for the reversible reversal taking into account the unknown parameter ϵ . We need to define three other parameters in order to normalize the field $\mu_0 H$ and the resistance $R(\mu_0 H, \alpha)$ of our experimental curves and obtain the relationship with h and $\cos^2 \omega$ of the model. The first two parameters to be determined are ΔR and R_\perp which allows to normalize the resistance values in the following way: $r = (R - R_\perp) / \Delta R$. The field values, in accordance with the model, must be normalized to the anisotropy field $\mu_0 H_a$, the third parameter. As we will see, these three parameters are obtained only from the experimental curve at $\alpha = 90^\circ$ provided two approximations are made. Two samples (A and B) have been chosen to reflect the observations made on all the other samples.

A. Reversible part

By representing the whole angular dependence measurement done at the maximum field of the magnet [Fig. 4(a)] as R vs $\cos^2 \alpha$, the experimental value of α is determined within an error of 1° [Fig. 5(b)]. Because of the unknown angle ϵ , the variation of resistance from this measurement may not give the total variation ΔR . Only the magneto-resistive curve at $\alpha = 90^\circ$ (equivalent to $\Omega = 90^\circ$) gives the real $\Delta R = R_0 - R_\perp$ with $R_0 = R(\mu_0 H = 0 \text{ T}, \alpha = 90^\circ)$ and $R_\perp = R(\mu_0 H \gg \mu_0 H_a, \alpha = 90^\circ)$ [see Eqs. (1) and (2)]. However, similar magneto-resistive curves are obtained around $\alpha = 90^\circ$ over a range of $2 - 3^\circ$ and each curve is not completely flat above $\mu_0 H_a$ [Fig. 4(b)] unlike the predictions of the model [Fig. 2(b)]. This discrepancy at $\alpha = 90^\circ$ could be explained by the fact that higher order terms in the magnetocrystalline (or uniaxial) anisotropy have been neglected in the model described in the appendix.²² This may also simply reflect the difficulty to perfectly well align the magnetization perpendicular to the wire axis due to, for example, some default acting as pinning center.

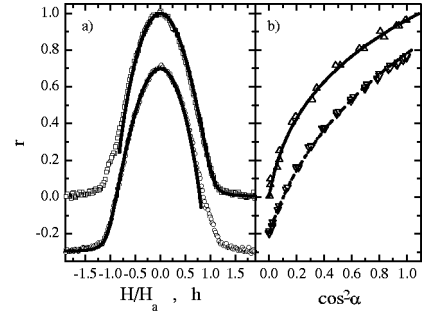


FIG. 5. (a) Normalized magneto-resistive curve $r = (R - R_\perp) / \Delta R$ vs $h = \mu_0 H / \mu_0 H_a$ for sample A at $\alpha = 90^\circ$ where $R_\perp = 257.6 \Omega$, $\Delta R = 4.05 \Omega$, and $\mu_0 H_a = 0.365$ T. For clarity, the up curve has been shifted by -0.3 . The full lines are the best curves obtained by comparison with the suggested model and corresponding to $\Omega = 92^\circ$. (b) Angular dependence $\cos^2 \alpha$ of normalized single Ni wires resistance at the maximum field of the magnet $\mu_0 H_{\max}$. The parameters of normalization for sample B (∇) are $R_\perp = 156.65 \Omega$, $\Delta R = 2.65 \Omega$, and $\mu_0 H_a = 0.34$ T. The curve for sample B has been shifted by -0.2 . The solid and dashed lines represent the angular dependence of the suggested model for the corresponding fixed $h_{\max} = \mu_0 H_{\max} / \mu_0 H_a$ taking into account the correction on Ω due to ϵ [see Eq. (3)]. The corrections are respectively, for samples A and B, $\cos^2 \epsilon = 0.92$ and $\cos^2 \epsilon = 0.97$.

Therefore a first approximation was made by defining R_\perp as the resistance at the maximum field for the curve at $\alpha = 90^\circ$, namely $R_\perp = R(\mu_0 H_{\max}, \alpha = 90^\circ)$. This value corresponds also to the minimum of the resistance in the angular dependence measured at saturating field (Fig. 4). Hence, we get $R_\perp = 257.6 \Omega$ and $\Delta R = 4.05 \Omega$ for sample A and $R_\perp = 156.65 \Omega$ and $\Delta R = 2.65 \Omega$ for sample B. The resistance of the experimental curve at $\alpha = 90^\circ$ was then normalized to $r = (R - R_\perp) / \Delta R$ in order to compare it with the curve at $\Omega = 90^\circ$ of the model. For that, the applied field of the experimental curve has to be normalized by the anisotropy field $\mu_0 H_a$. Because of the discrepancy discussed above, a second approximation was made in order to get this field. We observed that the changes in the width of the envelope of the experimental curves around $\alpha = 90^\circ$ were small. Thus, we considered to compare this envelope with the one of the theoretical curve at $\Omega = 90^\circ$. A value of $\mu_0 H_a = 0.365 \pm 0.005$ T was obtained for sample A and $\mu_0 H_a = 0.340 \pm 0.005$ T for sample B. Then, other curves of the model around $\Omega = 90^\circ$ may also be compared with our experimental curve at $\alpha = 90^\circ$. An excellent fit is obtained with the curve at $\Omega = 92^\circ$ [Fig. 5(a)] for sample A and at $\Omega = 88^\circ$ for sample B, without changing any of the three parameters. This justifies the two approximations mentioned above. Having fixed these three parameters for each sample, the other experimental curves may be normalized by these same parameters.

The first comparison between the model and the experimental data can be done on the angular dependence of the magneto-resistance at the maximum field of the magnet in the saturated regime. Because the magnetization of the wire should be along the field, we can check if the relation (1) and (2) may be really used to express the link between the resistance and the magnetization. Having determined the anisotropy field, the angular dependence of the model for the normalized maximum field $h_{\max} = \mu_0 H_{\max} / \mu_0 H_a$ may be

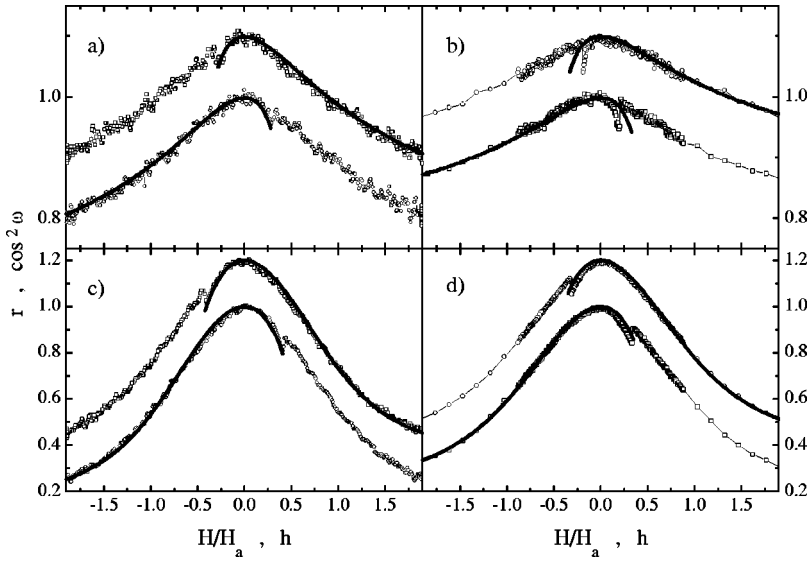


FIG. 6. Normalized magnetoresistive curves r vs h for the samples A and B at different values of α where $r = (R - R_{\perp}) / \Delta R$ and $h = \mu_0 H / \mu_0 H_a$. Their resistances at the maximum field ($\mu_0 H = 0.7$ T) are equal to, respectively, $R_{\perp} = 257.6 \Omega$ with a magnetoresistance of $\Delta R = 4.05 \Omega$ [(a) and (c)] and $R_{\perp} = 156.65 \Omega$ with $\Delta R = 2.65 \Omega$ [(b) and (d)]. Their anisotropy field has been fixed to $\mu_0 H_a = 0.365$ T and $\mu_0 H_a = 0.34$ T. For clarity, the down curves have been shifted by 0.1 for (a) and (b), and by 0.2 for (c) and (d). The full lines are the best curves obtained by comparison with the suggested model and the corresponding Ω value gives for (a) $\alpha = 34^{\circ} \rightarrow \Omega = 38^{\circ}$, (b) $\alpha = 30.5^{\circ} \rightarrow \Omega = 31^{\circ}$, (c) $\alpha = 74^{\circ} \rightarrow \Omega = 73^{\circ}$, and (d) $\alpha = 70.5^{\circ} \rightarrow \Omega = 70^{\circ}$.

compared with the experimental measurement for each sample. Taking into account the correction for Ω due to ϵ [see Eq. (3)], good agreement is found [Fig. 5(b)]. However, the sensitivity of such an analysis to determine ϵ is low, and large errors can occur. On the other hand, this agreement makes possible to continue the comparison on all the other experimental magnetoresistive curves. Again, a quite remarkable agreement is found between each experimental normalized curve (defined by α) and a curve of the model (defined by Ω) (Fig. 6). Nevertheless, in order to get a proof of the validity of our procedure, the obtained couple $(\cos \alpha, \cos \Omega)$ has to satisfy Eq. (3). An excellent linear fit is observed with the slope being $\cos \epsilon$ (Fig. 7). For all the samples, the ϵ values range between 10° and 20° close to the range provided by the manufacturer of membranes. The following parameters have been obtained for sample A and B : $\epsilon = (16.2 \pm 2)^{\circ}$ and $\epsilon = (10 \pm 4)^{\circ}$ respectively. This last result underlines the fact that a single Ni wire with diameter around 80 nm may be viewed as a single magnetic domain rotating uniformly with field from the saturation state to the remanent state. From the remanent state to the switching state (the jump in the magnetoresistive curves), depending on samples, deviations to the applied model may be observed [Figs. 6(b) and 6(d)]. These deviations are more pronounced at low angles α .

From the analysis presented above, nothing special in the extracted parameters, particularly from the ϵ value, may al-

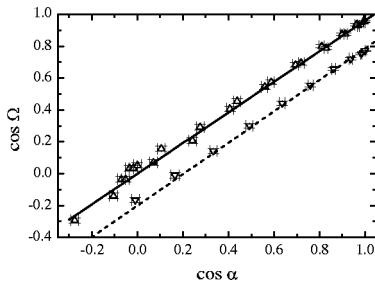


FIG. 7. Linearized relation between the angle Ω obtained from the applied model and the measured azimuthal angle α . The solid and dashed lines are linear fit to Eq. (3) with, respectively, for samples A and B, $\cos \epsilon = 0.96 \pm 0.01$ and $\cos \epsilon = 0.985 \pm 0.01$.

low us to distinguish between the samples in which the magnetization rotates uniformly up to the switching state and the others. We detect an apparent correlation between large anisotropy field and uniform rotation. Indeed, three samples may be really defined as showing a full agreement with the applied model. They are the ones, which have the highest values of the anisotropy field. The major part of the wire may be viewed as a single magnetic domain rotating uniformly. The deviations appearing in the magnetoresistive curves correspond then to some small parts of the wire having defaults acting as pinning center, for example.

The value of the anisotropy field of $\mu_0 H_a = 0.365$ T found for sample A can be analyzed in term of magnetic anisotropies. We consider a saturated magnetization for Ni bulk sample of $\mu_0 M_s = 0.6$ T.^{25,26} From Eq. (A2), a large uniaxial anisotropy of at least $K_1 = 1.55 \times 10^4$ (J/m³) is deduced. Such a value has already been observed and magnetostrictive effects associated with the strain due to the growth process were suggested.^{12,13} Another influence of stress on magnetic anisotropy K was also shown in a work of Jorritsma and Mydosh.²⁷

B. Irreversible part

The irreversible part of the magnetization reversal is observed in the magnetoresistive curves in the form of a jump (Fig. 6) at the so-called switching field. For the three samples showing an uniform rotation up to this field, the angular dependence of the switching field may be compared with the two known reversal modes, namely the Stoner-Wohlfarth and the Curling modes [Eqs. (A4) and (A8)]. These modes should only be applied when the magnetization is rotating uniformly before the irreversible jump. Having determined the value of ϵ , the experimental angle α is corrected to get the angular dependence of the switching field as a function of the angle Ω of the model. Then, by considering a saturated magnetization value of $\mu_0 M_s = 0.6$ T,^{25,26} an exchange length of $r_0 = 20$ nm⁴ and having fixed the value of the anisotropy field to $\mu_0 H_a = 0.365$ T deduced from our analysis of the magnetization reversal in the reversible regime

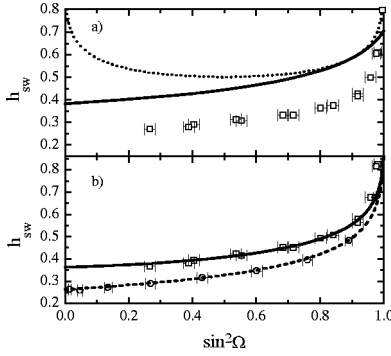


FIG. 8. Angular dependence of the normalized switching field $h_{sw} = \mu_0 H_{sw} / \mu_0 H_a$ for (a) sample A defined with its anisotropy field deduced from the reversible regime: $\square \mu_0 H_a = 0.365$ T. The dotted line represents the prediction for a Stoner-Wohlfarth mode reversal [Eq. (A4)]. The solid line represents the predictions for a Curling mode reversal [Eq. (A8)] with $S=2$ and $N_x=0.5$. The $S=2$ has been chosen considering a wire radius of $r=40$ nm and an exchange length of $r_0=20$ nm.⁴ (b) Samples A and B with lowered anisotropy fields in order to satisfy the prediction of a Curling reversal ($S=2$ fixed). The solid and dashed lines which fit the data points have been obtained, respectively, with the following parameters: $\mu_0 H_a = 0.27$ T with $N_x = 0.413$ and $\mu_0 H_a = 0.23$ T with $N_x = 0.408$.

(sample A), none of the two modes accounts for the angular dependence of the normalized switching field $h_{sw} = \mu_0 H_{sw} / \mu_0 H_a$ [Fig. 8(a)].

The angular dependence of the switching field in a single magnetic domain has already been addressed by several groups.^{7,9,12,28} In particular, relaxation measurements^{9,29} suggest that we need to consider that the irreversible magnetization reversal nucleates in a volume smaller than the whole magnetic volume. In this case, $\mu_0 H_a$ can be considered as different from the value taken for the reversible part. Then, the lower part of the angular dependence of the switching field may be well fitted considering a Curling mode with the following values: $\mu_0 H_a = 0.27$ T, $N_x = 0.413$, and $S=2$ [see Fig. 8(b)], as was suggested previously.¹² By allowing $\mu_0 H_a$ to be a free parameter, such analysis is applicable to all our samples. The result for sample B is $\mu_0 H_a = 0.23$ T, $N_x = 0.408$, and $S=2$ [Fig. 8(b)].

The idea of a nucleation has also been suggested by Braun³⁰ where he calculated the effect of the wire ends on the irreversible reversal and observed that the switching field was lowered due to such edge effects.

Considering then that the extracted parameters from the Curling mode in a smaller volume have a physical meaning with regards to the entire wire, the following picture for the reversal in the entire wire may be given.

From the demagnetization factor N_x ranging between 0.4 and 0.42 for all our samples, we suggest that, in the errors of our measurements, specially the wire diameter, the same small volume is involved in the irreversible reversal. This volume corresponds to an ellipsoid with short axis of the order of the wire diameter and a long axis of twice the short axis, as was previously suggested.¹²

From the anisotropy field deduced from the fit of the switching field to the Curling mode, a large induced uniaxial anisotropy K_1 is found and ranges between $K_1 = 2.0 \times 10^4$ (J/m³) and $K_1 = 3.2 \times 10^4$ (J/m³). This confirms the

observation done in the reversible regime with a deduced value of at least $K_1 = 1.55 \times 10^4$ (J/m³) for sample A.

By suggesting that the strain due to the growth process is identical along the wire, the deduced K_1 from the irreversible part may be subtracted to the anisotropy field deduced from the reversible part and a shape anisotropy is extracted. Such anisotropy ranges between 0.20 T and 0.22 T giving a demagnetization factor N_x varying between 0.445 and 0.455.

From this analysis and with the suggestions made, the magnetic volume which rotates uniformly is an ellipsoid with short axis around 80 nm and with its long axis 3 to 3.5 longer. So, we may consider the wire as a succession of such ellipsoid rotating coherently together, as it has been observed by Martin *et al.* in coupled Co dots.³¹ The large uniaxial anisotropy K_1 could be the factor insuring the uniform rotation.

Such a picture for the wire may also explain the deviations appearing in the magnetoresistive curves of some samples between the remanent and the switching field [Fig. 6(b) and 6(d)]. If the measured magnetoresistance of the wire corresponds to a mean value of the magnetoresistive contributions of each ellipsoid instead of a unique contribution of a long cylinder, this mean value could be lower if a certain number of ellipsoid have their long axis not fully aligned with respect to the wire axis. Such an effect would be more pronounced close to the switching field and for the low angles α .

IV. CONCLUSION

We were able to perform electrical contacts to single Ni nanowires. The anisotropic magnetoresistance measurements on these wires present a reversible part and an irreversible part of the reversal process. The reversible part can be accounted for by uniform rotation of the magnetization for any angle of the wire axis with respect to the applied field direction. The adjustment is precise enough that we can even detect the slight off-axis misorientation of the wire with respect to the field due to the membrane fabrication process. A big value for the anisotropy field $\mu_0 H_a$ is extracted and cannot be accounted for as arising from the shape of the wire. A large induced uniaxial anisotropy is found. The angular dependence of the switching field was also compared with the micromagnetic models of the uniform mode (Stoner-Wohlfarth model) and Curling mode. By using the information (particularly the large anisotropy field) gained from the analysis of the reversible part, we conclude that the observed angular dependence of the switching field cannot be accounted for by these modes. This is consistent with the notion that the irreversible reversal nucleates in a volume much smaller than the volume of the wire. In this case, a lower anisotropy field can be chosen and the Curling mode may describe the angular dependence of the switching field. Comparing the results gained from the reversible and irreversible parts, a single Ni wire may then be viewed as a succession of ellipsoid, with a mean magnetic volume defined by a short axis around 80 nm and a long axis around 250 nm, rotating uniformly because of the large uniaxial anisotropy.

ACKNOWLEDGMENT

This work has been supported in part by the Swiss National Science Foundation (Grant No. 20-55965.98).

APPENDIX: THEORETICAL SUMMARY

Considering an oblate spheroid with easy axis in the z direction, we define the angles ω and Ω as the orientations of the magnetization \vec{M} and the applied field $\mu_0\vec{H}$ with respect to the easy axis. The total energy density of this system is expressed by three terms: the Zeeman energy density, the shape anisotropy and the magnetocrystalline anisotropy approximated to the first order. This last term may also represent a general uniaxial anisotropy provided its axis is parallel to the easy axis of the spheroid. Stating that the equilibrium value of the magnetization at a fixed field is at the minimum of the total energy density, provides one equation:^{23,24,26}

$$2h \sin(\Omega - \omega) = \sin(2\omega), \quad (\text{A1})$$

where $h = \mu_0 H / \mu_0 H_a$, $\mu_0 H_a = 2K/M_s$, M_s is the saturation magnetization, and

$$K = K_1 + \frac{\mu_0 M_s^2}{2} (3N_x - 1), \quad (\text{A2})$$

with N_x , the demagnetization factor in the x direction and K_1 (or K_u), the anisotropy energy density factor.

Taking the inflection points of the total energy density, we get a second equation:

$$h \cos(\Omega - \omega) = -\cos(2\omega), \quad (\text{A3})$$

which gives, by combining with Eq. (A1), a relation between Ω and the switching field for the so-called Stoner-Wohlfarth mode, h_0 :

$$\sin^2 \Omega = -\frac{1}{h_0^2} \left(-\frac{1}{2} \pm \sqrt{\frac{4h_0^2 - 1}{12}} \right)^3. \quad (\text{A4})$$

Another reversal mode for the magnetization may be considered: the anisotropic Curling mode. Following Aharoni,²³ we replace Eq. (A3) by the following one:

$$h \cos(\Omega - \omega) = a \sin^2 \omega + b, \quad (\text{A5})$$

where

$$a = 1 + \frac{K_1}{2K} = \frac{3}{2} - \frac{1}{2} \frac{\mu_0 M_s}{\mu_0 H_a} (3N_x - 1) \quad (\text{A6})$$

and

$$b = \frac{\mu_0 M_s^2}{2K} \left(N_z - \frac{k}{2S^2} \right) - \frac{K_1}{K} = \frac{\mu_0 M_s}{\mu_0 H_a} \left(N_x - \frac{k}{2S^2} \right) - 1, \quad (\text{A7})$$

k is a numerical factor depending on the anisotropy,²³ and $S = r/r_0$ represents the reduced radius of the wires, r_0 being the exchange length.

By combining Eqs. (A1) and (A5), we get a relation between Ω and the switching field for the so-called Curling mode, h_1 :

$$\begin{aligned} \sin^2 \Omega = \frac{1}{h_1^2} [& -(1-a)^2 \cos^6 \omega_1 + (1-a)(1-3a \\ & - 2b) \cos^4 \omega_1 + (a+b)(2-3a-b) \cos^2 \omega_1 + (a \\ & + b)^2], \end{aligned} \quad (\text{A8})$$

with

$$\cos^2 \omega_1 = \frac{2a(a+b) - 1 \pm \sqrt{[1 - 2a(a+b)]^2 - 4(a^2 - 1)[(a+b)^2 - h_1^2]}}{2(a^2 - 1)}.$$

Unlike the case of the Stoner-Wohlfarth mode, the relation here between Ω and the switching field for the Curling mode, h_1 , depends on two parameters a and b or N_x and $k/2S^2$ if $\mu_0 M_s$ and $\mu_0 H_a$ are known.

*E-mail: yvan.jaccard@epfl.ch

¹J. F. Smyth, S. Schultz, D. R. Fredkin, D. P. Kern, S. A. Rishton, H. Schmid, M. Cali, and T. R. Koehler, *J. Appl. Phys.* **69**, 5262 (1991).

²A. Maeda, M. Kume, T. Ogura, K. Kuroki, T. Yamada, M. Nishikawa, and Y. Harada, *J. Appl. Phys.* **76**, 6667 (1994).

³K. J. Kirk, J. N. Chapman, and C. D. W. Wilkinson, *Appl. Phys. Lett.* **71**, 539 (1997).

⁴M. Lederman, R. O'Barr, and S. Schultz, *IEEE Trans. Magn.* **31**, 3793 (1995).

⁵A. Blondel, J. Meier, B. Doudin, and J.-Ph. Ansermet, *Appl. Phys. Lett.* **65**, 3019 (1994).

⁶K. Ounadjela, R. Ferré, L. Louail, J.-M. George, J. L. Maurice, L. Piraux, and S. Dubois, *J. Appl. Phys.* **81**, 5455 (1997).

⁷R. O'Barr and S. Schultz, *J. Appl. Phys.* **81**, 5458 (1997).

⁸Kimin Hong and N. Giordano, *Phys. Rev. B* **51**, 9855 (1995).

⁹W. Wernsdorfer, B. Doudin, D. Mailly, K. Hasselbach, A. Benoit,

J. Meier, J.-Ph. Ansermet, and B. Barbara, *Phys. Rev. Lett.* **77**, 1873 (1996).

¹⁰Y. Q. Jia, S. Y. Chou, and J.-G. Zhu, *J. Appl. Phys.* **81**, 5461 (1997).

¹¹A. O. Adeyeye, J. A. C. Bland, C. Daboo, and D. G. Hasko, *Phys. Rev. B* **56**, 3265 (1997).

¹²J.-E. Wegrowe, D. Kelly, A. Franck, S. E. Gilbert, and J.-Ph. Ansermet, *Phys. Rev. Lett.* **82**, 3681 (1999).

¹³J. Meier, B. Doudin, and J.-Ph. Ansermet, *J. Appl. Phys.* **79**, 6010 (1996).

¹⁴J. Meier, A. Blondel, B. Doudin, and J.-Ph. Ansermet, *Helv. Phys. Acta* **67**, 761 (1994).

¹⁵Poretics Corp., 111 Lindbergh Ave., Livermore, CA 94550-9520.

¹⁶I. Chlebny, B. Doudin, and J.-Ph. Ansermet, *Nanostruct. Mater.* **2**, 637 (1993).

¹⁷J.-E. Wegrowe, S. E. Gilbert, D. Kelly, B. Doudin, and J.-Ph. Ansermet, *IEEE Trans. Magn.* **34**, 903 (1998).

- ¹⁸J. Bass, in *Metals, Electronics Transport Phenomena*, Landolt-Bornstein, New Series, Group 3, Vol. 15a, edited by K. H. Hellwege and J. L. Olsen (Springer-Verlag, Berlin, 1982).
- ¹⁹T. R. McGuire and R. I. Potter, *IEEE Trans. Magn.* **11**, 1018 (1975), and references therein.
- ²⁰Th. G. S. M. Rijks, R. Coehoorn, M. J. M. de Jong, and W. J. M. de Jonge, *Phys. Rev. B* **51**, 283 (1995).
- ²¹E. C. Stoner and E. P. Wohlfarth, *Philos. Trans. R. Soc. London, Ser. A* **240**, 599 (1948) [reprinted in *IEEE Trans. Magn.* **27**, 3475 (1991)].
- ²²Referring to Aharoni (Ref. 23), we have considered the K_2 term and studied its influence on the envelope of the magnetoresistive curves. It was mainly to bend the curves around $\mu_0 H_a$. The change in the width of the envelope (giving $\mu_0 H_a$) induced by K_2 was less than 1%. Therefore, K_2 has been neglected by including its effect within our errors.
- ²³A. Aharoni, *J. Appl. Phys.* **82**, 1281 (1997); **30**, 70S (1959).
- ²⁴A. Aharoni, *Introduction to the Theory of Ferromagnetism* (Clarendon, Oxford, 1996), and references therein.
- ²⁵B. D. Cullity, *Introduction to Magnetic Materials* (Addison-Wesley, Reading, MA, 1972).
- ²⁶*Magnétisme, I-Fondements*, edited by E. du Trémolet de Lacheisserie (Presses Universitaires de Grenoble, Grenoble, 1999).
- ²⁷J. Jorritsma and J. A. Mydosh, *J. Appl. Phys.* **84**, 901 (1998).
- ²⁸S. Pignard, G. Goglio, A. Radulescu, L. Piraux, S. Dubois, A. Declémy, and J. L. Duvail, *J. Appl. Phys.* **87**, 824 (2000).
- ²⁹W. Wernsdorfer, K. Hasselbach, A. Benoit, B. Barbara, B. Doudin, J. Meier, J.-Ph. Ansermet, and D. Mailly, *Phys. Rev. B* **55**, 11 552 (1997).
- ³⁰H.-B. Braun, *J. Appl. Phys.* **85**, 6172 (1999).
- ³¹J. I. Martin, J. Nogués, I. K. Schuller, M. J. Van Bael, K. Temst, C. Van Haesendonck, V. V. Moshchalkov, and Y. Bruynseraede, *Appl. Phys. Lett.* **72**, 255 (1998).